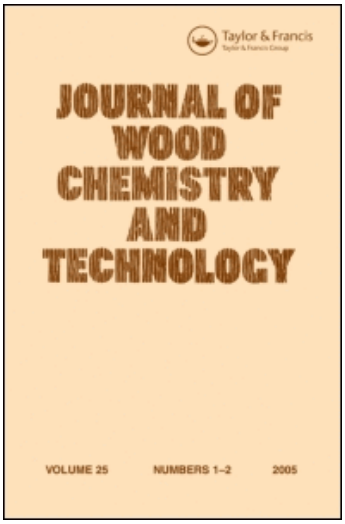

Journal of Wood Chemistry and Technology
Publication details, including instructions for authors and subscription information:
http://www.informaworld.com/smpp/title~content=t713597282

Yellowing Mechanism and Kinetics of Thick Handsheets of Softwood Thermomechanical Pulp

Sylvain Robert[a]; Claude Daneault[a]; Xiaoqi Pan[a]; Arthur J. Ragauskas[a]
[a] Centre de Recherche en Ptes et Papiers Université du Québec à Trois-Rivières C.P. 500, Trois-Rivières, Québec, Canada

To cite this Article Robert, Sylvain , Daneault, Claude , Pan, Xiaoqi and Ragauskas, Arthur J.(1995) 'Yellowing Mechanism and Kinetics of Thick Handsheets of Softwood Thermomechanical Pulp', Journal of Wood Chemistry and Technology, 15: 1, 113 — 133
To link to this Article: DOI: 10.1080/02773819508009502
URL: http://dx.doi.org/10.1080/02773819508009502

JOURNAL OF WOOD CHEMISTRY AND TECHNOLOGY, 15(1), 113-133 (1995)

YELLOWING MECHANISM AND KINETICS OF THICK HANDSHEETS OF SOFTWOOD THERMOMECHANICAL PULP

Sylvain Robert and Claude Daneault
Centre de Recherche en Pâtes et Papiers
Université du Québec à Trois-Rivières
C.P. 500, Trois-Rivières, Québec, Canada, G9A 5H7

ABSTRACT

Two major UV absorption peaks were observed when thermomechanical papers (black spruce, balsam fir) were exposed to a UV light in the range 300-400 nm for up to 65 hours. One of the peaks around 425 nm was the result of the formation of three different chromophores. The other one at 360 nm was a composite band resulted from the disappearance of one chromophore, and the appearance of a different chromophore, which seemed to be the intermediate molecule of two steps photoinduced reaction. The kinetic observed always follows a first order reaction rate. We believe that the two chromophores observed at 360 nm were related to the formation of the chromophores appearing at 425 nm. This resulted in a system of four chromophores which occurred in yellowing involving three reaction pathways. One of the reaction involved a chromophore which was affected by peroxide and borohydride bleaching. The elimination of this chromophore by either oxidation or reduction minimized its effect on color reversion. The other reaction pathways could also be modulated either by borohydride or peroxide. One of the major problem in using thick handsheets is highlighted.

Introduction

Over the last few years, studies were conducted to determine the mechanisms involved in yellowing of papers. At least two different pathways produce yellow products containing quinoid structures. These products are the result of photochemical reactions with lignin. The study of one pathway appears in Lebo *et al* [1], who found that 75% of the colored structures are *o*-quinones. Two decades earlier, Leary [2] proposed that the phenolic hydroxyl groups of lignin are the site of the

yellowing reaction, and that these groups are responsible for the light absorption and/or the phenolic hydrogen transfer with radical or excited molecules. Later, Lin and Kringstad [3,4] showed that the α-carbonyl group of the chromophores of lignin are responsible for the UV absorption. They later concluded that the α-carbonyl group is responsible for the abstraction of phenolic hydrogen.

Brunow and Sivonen [5] showed that the excited α-carbonyl group transfers its energy to oxygen, from triplet to singlet. Matsuura *et al* [6] found that singlet oxygen oxidizes the phenolic group in lignin to produce a phenoxide radical.

Phenoxide radicals are known to lead to yellow quinoid structures. The first mechanism involves the abstraction of an phenolic hydrogen by singlet oxygen or by an excited α-carbonyl group and leads to a phenoxide radical.

Another mechanism proposed by Gierer and Lin [7] involves a cleavage of non-phenolic phenacyl-α-O-aryl-ether to phenacyl-phenoxy free radical pairs. Further reactions with oxygen and/or other lignin functional groups lead to colored chromophores.

Recent studies on ultra-thin sheets of black spruce TMP [8] showed that UV-Visible spectra of near-UV irradiated bleached TMP caused the formation of two major absorption peaks with $\lambda_{max} \approx 410$ and 330 nm. The 330 nm peak is associated with the formation of aromatic ketones, while the 410 nm peak is associated with quinones.

On the other hand, the bleaching studies of Holah and Heitner [9] on SGW and TMP have clearly shown that under the attack of hydrogen peroxide, a decrease in the absorption spectrum at $\lambda_{max} = 358$ nm can be attributed to the reaction of the coniferaldehyde element of lignin with the OOH^- ion. Also, an observed decrease in the 420-500 nm region is interpreted as a transformation of quinones in carboxylic acids upon reaction with the OOH^- ion.

Recently, Holbom *et al* [10] have shown that lignin from stone groundwood is photodegraded mainly by α- and ß-aryl cleavage of coniferaldehyde type structures around 360 nm leading to the formation of degradation products with aliphatic and aromatic aldehyde, ketone and carboxyl groups. Phenylcoumaran was also degraded, possibly to stilbene structures. Demethoxylation of the structures also take place.

All these various experiments indicates that the culprits of the photoyellowing process are the phenolic hydroxyl and coniferaldehyde groups. However, the exact mechanism of the photoyellowing process is not totally understood, but some suggest that it involves the reaction of a carbon centered radical, possibly in α of the aromatic ring [11-12].

The purpose of this work is to further elucidate the mechanism of yellowing. Kinetics of yellowing of thick unbleached, peroxide bleached and borohydride bleached TMP handsheets of a balsam fir-black spruce mixture were studied using long exposure time to UV light.

Materials and methods

Thermomechanical pulp containing 25% balsam fir (*Abies balsamea*) and 75% black spruce (*Picea mariana*). The chips were provided by Kruger Inc. (Trois-Rivières, Québec) and sorted with a Rader model M-2215 classifier. TMP pulp was prepared according to the following procedure. Chips were washed with fresh water and steamed for 6 minutes at 151 kPa. They were refined in a one-stage process with a CD300 Sunds Defibrator refiner at the Université du Québec à Trois-Rivières. The specific energy was 2398 kWh/ADMT (air dried metric ton). The pulp was then washed with fresh water and thickened to about 20% consistency. It had a freeness of 110 mL and a brightness of 57.6% ISO. The pulp used for control experiments was used as prepared, and stored at 4°C in light-sealed polypropylene bags.

The pulp (20 g of air-dried) was pretreated with 0.4% Na_5DTPA (sodium diethylenetriaminepentaacetate) to complex the undesirable heavy metal ions. This treatment was undertaken at 60°C for 15 minutes at 0.3% pulp consistency. The initial pH was about 6.1±0.2.

To obtain a one stage hydrogen peroxide bleached pulp (P-TMP) we used the following procedure. We used 0.05% magnesium sulfate ($MgSO_4 \cdot 7H_2O$) and 3% of sodium silicate (Na_2SiO_3, 41° Be) to help stabilize hydrogen peroxide through the formation of peroxysilicates. Then 2% hydrogen peroxide solution was added. The pH was set at 11.0 with NaOH, and the consistency adjusted to 15% with deionized water. The temperature was raised to 70°C, and held for 2 hours. Con-

sumption of peroxide was 1.97% (0.03% of residual hydrogen peroxide) as determined by iodometric titration. After bleaching, we neutralized the mixture with sodium pyrosulfite ($Na_2S_2O_5$) at 3% consistency to obtain a pH of 5.5. Deionized water was used for washing and, following the treatment, the pulp was filtered and thickened.

To prepare a sodium borohydride bleached pulp (B-TMP) we used the following procedure. We added a 0.3% $NaBH_4$ solution to a pulp. The pH was set at 11.0 with NaOH, and the consistency adjusted to 6% with deionized water. The temperature was raised to 70°C, and held for 30 minutes. After bleaching, we neutralized the mixture with sodium pyrosulfite ($Na_2S_2O_5$) at 3% consistency to obtain a pH of 5.5. Deionized water was used for washing and, following the treatment, the pulp was filtered and thickened.

There are two different methods that can be used to obtain reflectance spectra of handsheets. First, you can use low-basis weight (≈ 10 g/m^2) handsheet and obtain homogeneous chromophore concentration throughout the sheet upon irradiation. By doing this, you can take measurements over white and black background and use the Kubelka-Munk analysis:

$$F(R_\infty) = \frac{k}{s} = \frac{(1 - R_\infty)^2}{2R_\infty} \qquad (1)$$

where k is the specific absorption coefficient and s is the scattering coefficient.

A second technique uses homogeneous high-basis weight (> 60 g/m^2) handsheets. Johnson [13] has shown that for papers thicker than 30 g/m^2, for a given wavelength, the change in the scattering coefficient, s, is very small and can be approximate as a constant. Upon irradiation and photoyellowing, you may assume that the scattering coefficient in the Kubelka-Munk equation remains constant, thereby obtaining a more direct relation between the absorption coefficient, k, and the reflectance of the handsheet. Using very high basis weight handsheet (200 g/m^2), one can simplify the relationship and use the simpler Beer-Lambert absorption law.

We have decided to use this second approach, and thus postulate that the absorption spectra of the handsheets that we will measure will be directly related to the concentration of the chromophores within the handsheet. This relationship is only

correct when the distribution of chromophores is exponential within the thickness of the paper sample accessible to the light source of the spectrophotometer [14,15,16].

It should be noted however, that this relationship may not necessarily be constant. It is possible that, at high UV exposures, the distribution of chromophores through the thickness of the sheet may not remain exponential, the surface of the paper becoming saturated with chromophores. If this append, one will observe a saturation of the signal with time. Care should thus be taken in the evaluation of the results. The behavior that will be observed will not represent the whole photoyellowing process that will take place within the exposed handsheet, but it will be what the observer perceived as the yellowing of a thick handsheet. Results will thus be compared to those observed in literature for very thin (10 g/m^2) handsheets.

Considering what have just been said, all handsheets were prepared from pulps according to CPPA Standard Method C.5 (≈ 200 g/m^2 handsheets).

Optical properties were measured on a photoelectric reflectance photometer (Technibrite Micro TB-1C) according to CPPA Standard Method E.1 and E.2. The color descriptions used the CIE L*a*b* color space; a uniform three-dimensional color scale developed for opaque diffuse objects and designed to simulate visually adjusted spacing of surface colors.

The CIE L* axis is a representation of the whiteness of light reflected from the paper. The CIE a* axis represents the opposing green-red color vector, with a positive value directed toward red. The CIE b* axis represents the blue-yellow opposition color vector, with yellow on the positive side. This last vector uses measurements made with two wavelengths, 455 and 557 nm; the blue-violet and yellow-green parts of the visible spectrum. In this paper, only initial and final L*a*b* coordinates will be presented for comparison, because the analysis used for the kinetics use full UV-Visible spectra.

UV-Visible spectra were recorded on a Cary 3 spectrophotometer from Varian equipped with a 73 mm integrating sphere ($BaSO_4$ coated, side-on R928 PMT detector). This setting allows us to take diffuse reflectance measurements of the handsheets. The reflectance (R_∞) is then converted in absorbance (Abs) with the following expression derived from the Beer-Lambert law: $Abs = - \log R_\infty$

Accelerated aging was performed with a Rayonet photochemical reactor (Southern New England Ultraviolet Co., Hamden, Connecticut) using RPR-3500Å lamps. These lamps have a pseudo Gaussian output of approximatively 24 watts between 300 and 420 nm centered at 350 nm. The output rate is about 1.5 to 5 $\times$ 10^{16} photons/sec/cm^3, resulting to about 9,200 μW/cm^2 at reactor center. The sheets were exposed to UV light from 1 second to 65 hours, allowing us to monitor short and long term kinetics.

The resulting spectra were averaged from five different test handsheets.

Results and discussion

The results of yellowing for a total irradiation time of 65 hours for TMP, P-TMP and B-TMP are presented in Table 1. This table shows the usual CIE L*a*b* coordinates along with the spectroscopic data of the maximum of the difference spectra taken for the samples (detailed later). Following discussion will show why the analysis of the first four columns only can be tricky and lead to false evaluations. They are nevertheless included here for comparison.

Figure 1 shows a typical absorption spectrum for an unbleached TMP sample taken after various irradiation times. Overexposed on these spectra is the hatched shape of the emission of the excitation lamp in no specific units.

The difference spectra from these curves shows two major absorption peaks appeared around 360 and 425 nm (as shown in Figure 2, with overexposed on these spectra is the hatched shape of the emission of the excitation lamp in no specific units). As noted before, the peak observed around 360 nm is generally assumed to come from a reaction of the coniferaldehyde moiety in lignin, while the one around 425 is assumed to come from the generation of quinones [9,17]. The time behaviors of the maximum of absorption bands are shown for unbleached TMP at 430 nm in Figure 3 and at 362 nm in Figure 4.

An analysis of absorption peaks located below 330 nm was not performed. In the literature, at least 3 research groups have noted an increase of absorption around 330 nm [18,19,20,21].The absence of such an observation in the present work is not surprising considering that the sample, due to its thickness, absorb most of the light

TABLE 1

ISO Brightness and CIE L*a*b* for TMP, B-TMP and P-TMP

	ISO Brightness	*CIE L**	*CIE a**	*CIE b**	A_{360}	A_{425}
Unirradiated pulps						
TMP	57.67	87.27	0.50	12.21	1.030	0.425
B-TMP	64.06	89.14	0.02	9.40	0.860	0.390
P-TMP	71.37	93.61	-1.01	10.91	0.905	0.330
Yellowed pulps (65 hours in Rayonet)						
TMP	30.83	80.90	3.24	32.62	1.017	0.732
B-TMP	32.94	81.09	2.00	29.91	1.047	0.730
P-TMP	33.46	83.10	2.28	32.66	1.015	0.703

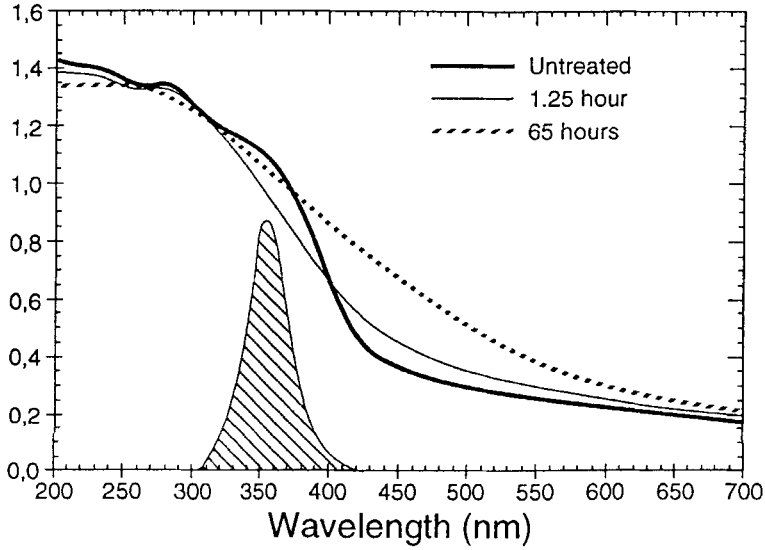

FIGURE 1. Absorption spectra of an unbleached TMP handsheet after 0, 1.25 and 65 hours of photoyellowing. Overexposed on these spectra is the hatched shape of the emission of the excitation lamp in no specific units.

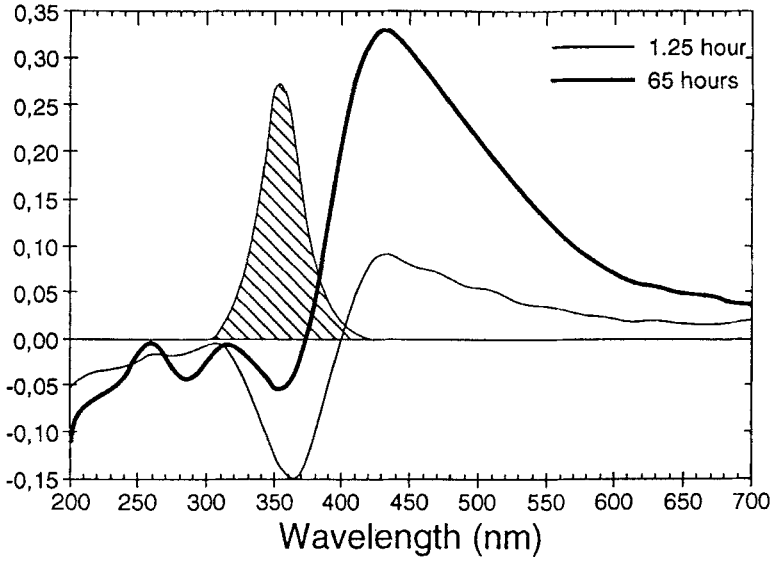

FIGURE 2. Absorption difference spectra of an unbleached TMP handsheet after 1.25 and 65 hours of photoyellowing. Overexposed on these spectra is the hatched shape of the emission of the excitation lamp in no specific units.

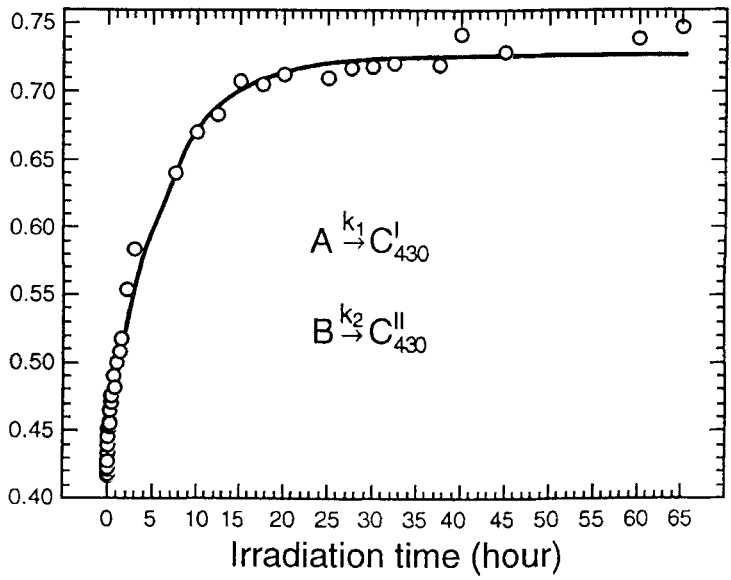

FIGURE 3. Variation of the absorption difference spectra at 430 nm for unbleached TMP.

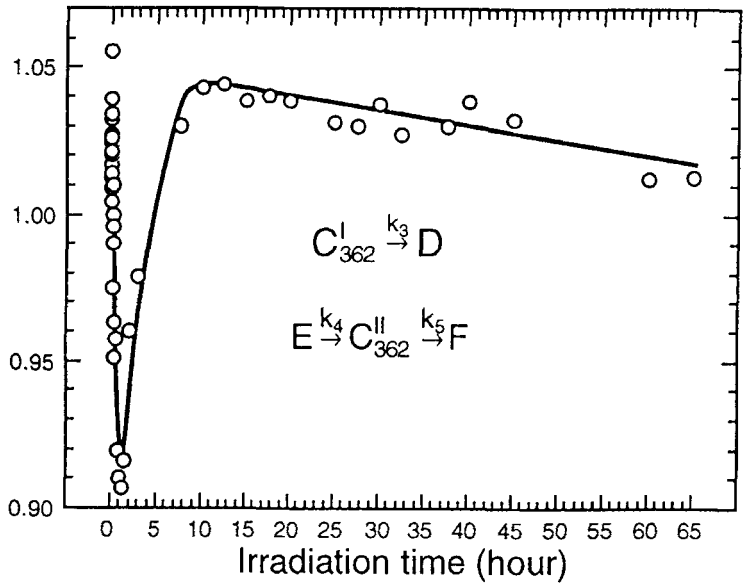

FIGURE 4. Variation of the absorption difference spectra at 362 nm for unbleached TMP.

below 340 nm because of the high lignin content (between 27 and 29%). This results in a very rapid decrease in the signal to noise ratio, so any interpretation of these absorption bands and kinetics curves was unreliable. The use of these bands could lead to artifacts, and was thus ignored.

A statistical program (SAS Release 6.03 from SAS Institute Inc., Cary, NC, USA running on a RS/6000 computer) was used to calculate the nonlinear curve fitting of these kinetic using the Marquardt's algorithm [22]. We have tried to use as few reaction pathways as possible for the evaluation of curve fitting, keeping the interpretation as simple as possible. Combinations of 1 to 3 reactions with first or second order reaction rate were tested. In all cases, the use of two simple first order reactions was sufficient to fit all data at 430 nm and three first order reactions was enough to fit all data at 360 nm. The analysis of the residues of calculations for the 362 and 430 nm peak of unbleached TMP is shown in Figure 5, as an example of our worst results. All our results were fitted with the same method, and in all other

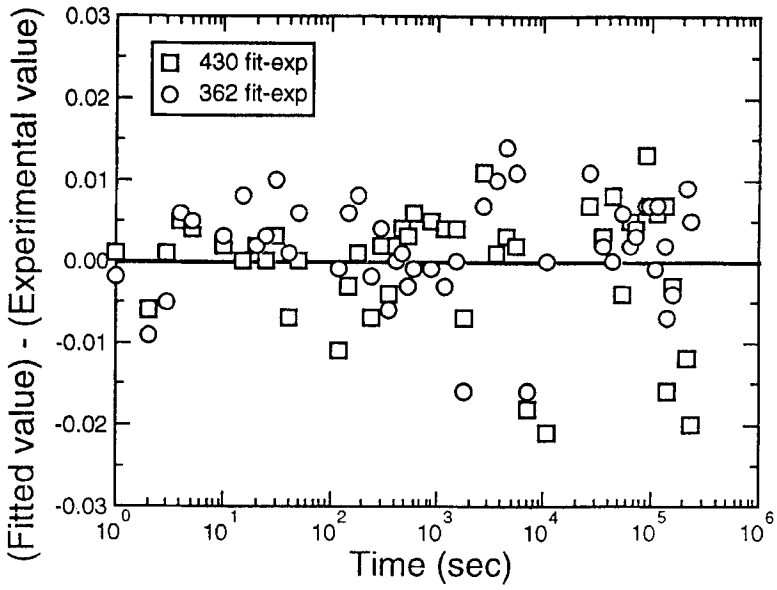

FIGURE 5. Residues of curve fitting from the time behavior of the 362 and 430 nm absorption band for unbleached TMP.

cases with better correlation than the one shown. From the uniform scattering of the observed values around the ideality line we can conclude that our curve fitting calculations are correct, and thus the kinetic equations that we have extracted from these results. All experimental data were fitted with the same technique and yield the same correlation between the experimental data and the calculated curve.

The behavior of the 430 nm peak can easily be fitted with the juxtaposition of two growing exponential, resulting in two parallel chemical reactions creating two different chromophores that absorbed in this spectral region, as expressed in Figure 3. It is also theoretically possible that these two reactions are consecutive; the mathematics cannot distinguish between these two possibilities. However, without proof of consecutive reactions, we posit the hypothesis that these reactions are parallel. If they are in the future discovered to be consecutive, the kinetics will be simplified. Thus, we do not have the right to assume that chemical specie B is the same as chromophore C^{I}_{360}.

The 362 nm peak, on the other side, can only be fitted by the destruction of one chromophore in one reaction, and the creation of an intermediate, which when its concentration is high enough, disappears to give birth to another chromophore in a second chain reaction, as expressed in Figure 4. Figure 6 shows the decomposition of the 362 nm absorption band. The rapid fall in absorption can be attributed to a fast degradation of one chromophore. The second curve showing an increase in absorbance, followed by a slow decrease, is characteristic of the formation of an intermediate, followed by its decomposition. It should be noted that the decrease in absorption around 360 nm has already been shown in the literature [23,24] and was linked to the induced photobleaching by irradiation with light around 420 to 430 nm.

Based on the behavior of the curves in Figures 3, 4 and 6, the following chemical equations for the yellowing of these two peaks for unbleached TMP can be extracted:

$$A \xrightarrow{k_1} C^{I}_{425} \tag{2}$$

$$B \xrightarrow{k_2} C^{II}_{425} \tag{3}$$

$$C^{I}_{360} \xrightarrow{k_3} D \tag{4}$$

$$E \xrightarrow{k_4} C^{II}_{360} \xrightarrow{k_5} F \tag{5}$$

where, A to F refers to the various chemical moieties involved in the yellowing process. C^{X}_{nm} indicates the chromophores responsible for the behavior of the absorption peak itself.

From these chemical equations' reactions, we can derive the following first order kinetics equations:

$$\frac{d\,C^{I}_{425}}{dt} = k_1 A \tag{6}$$

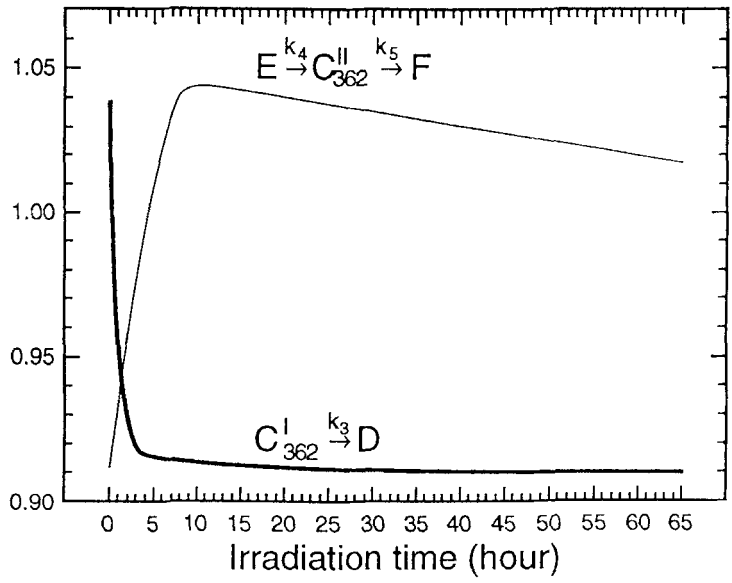

FIGURE 6. Decomposition of the observed kinetic observed at 362 nm for the unbleached TMP.

$$\frac{d\,C^{II}_{425}}{dt} = k_2\,B \tag{7}$$

$$\frac{d\,C^{I}_{360}}{dt} = -\,k_3\,D \tag{8}$$

$$\frac{d\,C^{II}_{360}}{dt} = k_4\,E - k_5\,F \tag{9}$$

In all cases, what is measured experimentally is absorption. It is related to concentration by the molar absorptivity coefficient, ε, which is unknown, and not necessarily the same for all chromophores involved in the yellowing process. By proposing that $\boxed{\text{Abs} = \varepsilon \times \text{Conc}}$, from the kinetics equations *6* to *9*, and by the minimizing the mathematical equations and errors in the various models, we extract the following solved equations for unbleached pulps.

$$Abs_{425} = \varepsilon^{I}_{425} A_0 \left(1 - e^{-k_1 t}\right) + \varepsilon^{II}_{425} B_0 \left(1 - e^{-k_2 t}\right) + Abs^{I,II}_{425,t=0} \quad (10)$$

$$Abs_{360} = Abs^{I}_{360,t=0} e^{-k_3 t} + \frac{\varepsilon^{II}_{360} k_4 E_{t=0}}{k_5 - k_4} \left(e^{-k_4 t} - e^{-k_5 t}\right) + cte \quad (11)$$

Difference spectra of other pulps, bleached with peroxide or borohydride, show absorption bands like the one shown in Figure 2. However, the position of the maximum shifts slightly as a function of time, as shown in Figure 7 for the unbleached TMP. The two absorption bands are very close and wide, as seen in Figure 2. Thus, they will influence each other regarding the exact position of the maxima observed in Figure 2. Also, it is difficult to obtain exact reproducibility in the position of the absorption peak for the first 20 seconds because the changes in the reflectance spectra are very small, and the signal to noise ratio is then rather low. This explains the variation in the position of the peak for the first 20 seconds. As the time increases, the position of the peak can be located with more precision. The exact position of these maxima also varies slightly from one type of pulp to another (TMP, P-TMP and B-TMP). The behavior of all pulps is shown in Figures 8 and 9 around the 425 and 360 nm absorption peak, respectively. From now on, we will therefore refer to the 425 and 360 nm absorption bands.

From Figure 9, it is clear that unbleached pulp behaves differently than bleached pulps. In both peroxide and borohydride bleached pulps, k_5 (the speed constant of the reaction $C^{II}_{360} \rightarrow F$) turns out to be negligible. It means that equations (*9*) and (*11*) can be simplified for both peroxide and borohydride bleached pulps as:

$$\frac{d\,C^{II}_{360}}{dt} = k_4 E \quad (12)$$

$$Abs_{360} = Abs^{I}_{360,t=0} e^{-k_3 t} + \varepsilon^{II}_{360} E_{t=0} \left(1 - e^{-k_4 t}\right) + cte \quad (13)$$

In these equations, the "cte" and $Abs^{I,II}_{425,t=0}$ at 425 nm (Equations *10* @ *13*) are proportional to the initial absorbance of the spectral curve. The various coefficients of the equations 6 to 13 are presented in Table 2.

Considering that the 360 nm peak is associated with coniferaldehyde type groups, and that the initial absorbance at 360 nm is lower with either H_2O_2 or $NaBH_4$, as shown in Table 1, we conclude that the "concentration" of this later

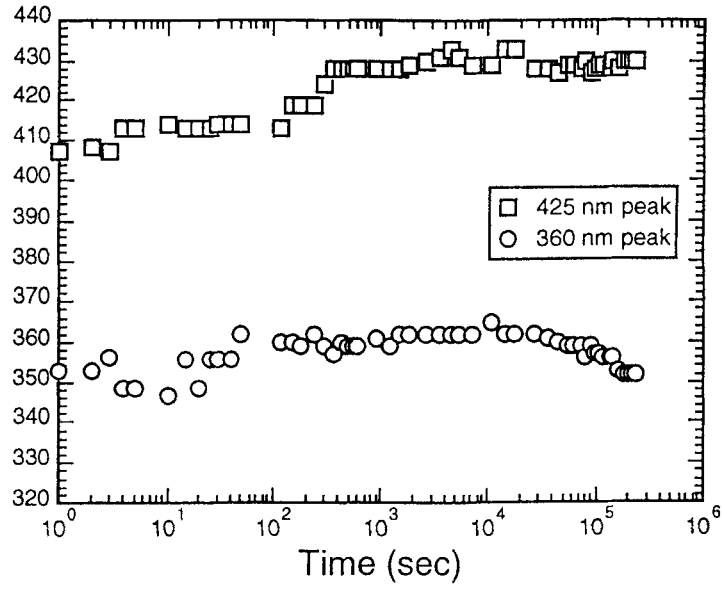

FIGURE 7. Position of the absorption peak as a function of irradiation time for unbleached TMP.

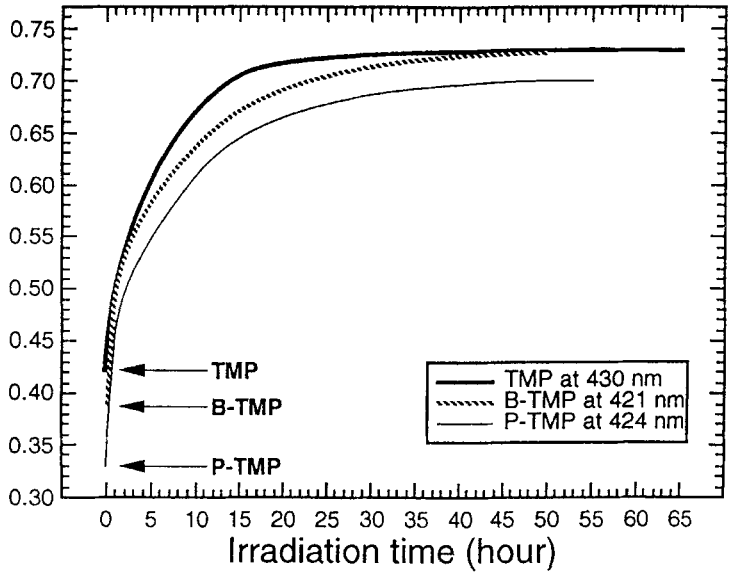

FIGURE 8. Kinetics of the 425±5 nm absorption band for all three pulps studied.

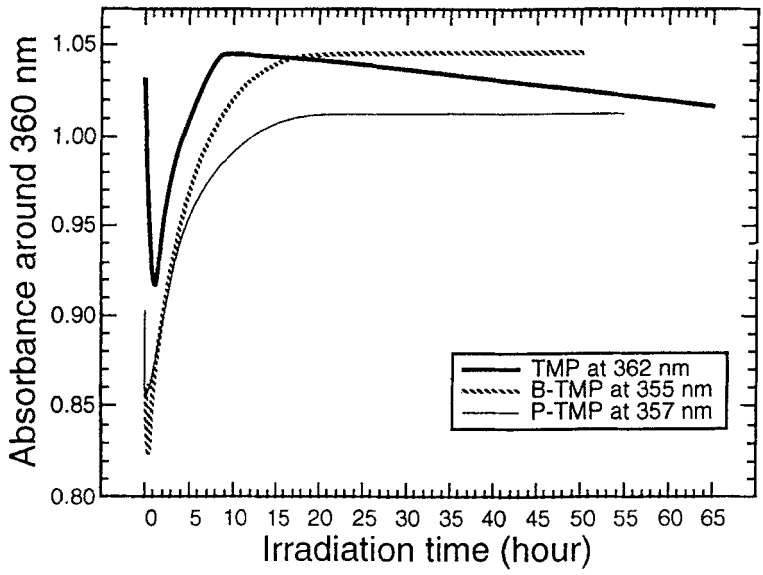

FIGURE 9. Kinetics of the 360±5 nm absorption band for all three pulps studied.

chemical is decreased in both bleached pulps. This is interpreted as the result of the reaction of both bleaching chemicals with chromophore C^{I}_{360}. Since the initial absorbance is lower, it is interpreted as a decrease of the real concentration of the chromophore responsible for the absorption by either its destruction (and possible removal since bleaching is known to decrease yield and increase mechanical properties), or by modifying the chromophore enough to change its molar absorptivity.

Initial absorbance at 425 nm also indicates the efficiency of both H_2O_2 and $NaBH_4$ in eliminating quinones from pulps; H_2O_2 being better than $NaBH_4$. Usually the quinones are oxidized to carboxylic acids by hydrogen peroxide, while borohydride reduces them to hydroquinones. It seems however that the reaction of borohydride with quinolic groups does not generate coniferaldehyde groups similar to those found in the unbleached TMP because the shape of the initial reflection spectrum in the 360 nm region is different and the initial absorption (A_{360}) is lower than what is found in unbleached TMP.

TABLE 2

Kinetics Coefficients for TMP, B-TMP and P-TMP According to Equations 10 to 13, at 425 and 360 nm

	Unbleached (*10-11*)	Borohydride (*10-13*)	Peroxide (*10-13*)
At 360 nm:			
k_3 (h^{-1})	1.19 ± 0.06	50 ± 15	65 ± 20
k_4 (h^{-1})	$9 \times 10^{-4} \pm 2 \times 10^{-4}$	0.22 ± 0.01	0.21 ± 0.02
k_5 (h^{-1})	0.62 ± 0.03	negligible	negligible
$Abs^{I}_{360\,.\,t=0}$	0.5117 ± 0.0009	0.041 ± 0.005	0.058 ± 0.006
$\varepsilon^{I}_{360} \bullet E_{t=0}$	$76 \times 10^{-5} \pm 3 \times 10^{-5}$	0.218 ± 0.004	0.171 ± 0.005
cte	0.5112 ± 0.0007	0.820 ± 0.003	0.843 ± 0.003
R^2_{360}	0.9620	0.9883	0.9723
At 425 nm:			
k_1 (h^{-1})	10 ± 3	1.6 ± 0.3	1.2 ± 0.1
k_2 (h^{-1})	0.158 ± 0.009	0.081 ± 0.008	0.073 ± 0.007
$\varepsilon^{I}_{425} \bullet A_{t=0}$	0.264 ± 0.005	0.220 ± 0.009	0.23 ± 0.01
$\varepsilon^{II}_{425} \bullet B_{t=0}$	0.041 ± 0.005	0.13 ± 0.01	0.16 ± 0.01
$Abs^{I\text{-}II}_{425\,.\,t=0}$	0.422 ± 0.002	0.387 ± 0.002	0.322 ± 0.002
R^2_{425}	0.9962	0.9946	0.9968

From the evaluation of k_5 and the shape of the curves of Figure 9 for bleached pulps, we clearly observe the formation of one chromophore, but this chromophore does not behave as a reaction intermediate as shown for unbleached pulp. If the chromophores responsible for the 360 nm absorption are roughly the same for all pulps, we conclude that the bleaching (with peroxide or borohydride) has modified the initial species "E" enough to completely inhibit the second part of the reaction (*9*). However, this modification of "E" was not strong enough to significantly modify the molar absorptivity of C^{II}_{360}.

The rate constants (k_1 to k_5) are very similar for both bleached pulps while those measured for unbleached pulps shows major differences. This implies that the chemical environment is very different between a bleached and an unbleached pulp.

This difference in chemical environment will influence the rate constant measured for all reactions involved in the photoyellowing process. Because of this, one cannot compare the values on the same row in Table 2. However, the relationships observed across a column can be qualitatively compared to the relationships in another column.

In all cases, the observed values of k_4 for B-TMP and P-TMP, and those of k_4 and k_5 for the unbleached TMP are much lower that the value of k_3. These rate constants' k_4 and k_5 are thus assigned to a slow reaction, while k_3 is assigned to a fast reaction. The same comparison can be made for k_1 and k_2. For this reason, we believe that the rate constant k_1 is related to k_3 and the rate constant k_2 is related to k_5. In both bleached pulps, the value of k_5 becomes negligible because of the increased rates of the constant k_3 and k_4, resulting in a non detectable rate constant.

We posit the following hypothesis for the global reaction mechanism for color reversion as observed in our experiments of thick handsheets (equations *14* and *15*). The dashed arrows indicate the hypothetical relationship between the two systems at 360 and 430 nm. Thus, from the observed behavior of these thick handsheets, there is a possibility that the species "A" and C^{I}_{360} are the same, "B" would be C^{II}_{360}, "D" would be C^{I}_{425} and "F" would be C^{II}_{425}.

$$C^{I}_{360} \xrightarrow{k_3} D \cdots\cdots\blacktriangleright A \xrightarrow{k_1} C^{I}_{425} \qquad (14)$$

$$E \xrightarrow{k_4} C^{II}_{360} \xrightarrow{k_5} F \cdots\blacktriangleright B \xrightarrow{k_2} C^{II}_{425} \qquad (15)$$

It should also be noted that species "E" does not absorb light in the 360 nm absorption band. It may however absorb in the 300-350 nm region covered by the emission lamps. But, as we pointed out, an analysis of absorption peaks located below 330 nm was not performed due to its thickness, absorb most of the light below 340 nm because of the high lignin content. This is very unfortunate, and shows one of the major problems of using thick handsheets. A complete comparison of the

yellowing kinetics of various basis weight samples should also be undertaken. In this way, it will probably be possible to link these kinetics equations to the chemical structures recently proposed in the literature for the formation of arylglycerol-β-arylether ketyl radicals and their subsequent cleavage to form phenoxy radicals and aromatic ketones [12].

Since the 360 nm peak is generally associated with coniferaldehyde groups this result implies that there are other types of lignin sub-structures responsible for the color reversion phenomenon. It should be emphasized here that the leucochromophore "E" is probably different in all three kinds of pulps because many moieties present in lignin can absorb light in the 300-350 nm region.

For both bleached pulps, the observed values of rate constant are about the same. Since the chemicals responsible for the bleaching are totally different, an oxidizer and a reducer, this implies that the resulting chromophores present in pulp before color reversion have different structures. Because the initial absorbance at 360 nm are different, it is unfortunately impossible to evaluate if it is the result of a lower concentration or a different molar absorptivity. Other experiments are needed to settle this question.

The results indicates, nevertheless, that we observe color reversion in three totally different chemical environments. Both bleached pulps show similar behavior for the disappearance of the 360 nm band. The unbleached pulp shows the formation of a reaction intermediate, that was absent from both bleached pulps. Surprisingly, borohydride bleached pulp seems to exhibit a long term yellowing that reaches a similar degree of formation of quinolic structures at 425 nm (A_{425} = 0.730) compared to the unbleached pulp (A_{425} = 0.732), while the yellowing of the peroxide bleached pulp results in a lower amount of quinones formed (A_{425} = 0.703). But, one should note that the initial absorption at 425 nm is 0.6 absorbance unit lower for P-TMP than for B-TMP. This indicates a better removal of quinones by peroxide bleaching than by borohydride. Thus the increases in the absorption peak at 425 nm are 0.340 for B-TMP and 0.373 for P-TMP.

This indicates that the amount of quinolic structures produced by yellowing of the peroxide bleached pulp is greater than the amount generated on B-TMP. This can be explained by the fact that the initial absorption at 360 nm is greater for

P-TMP (0.905) than for B-TMP (0.860). Because the residual amount of phenolic hydroxyl and coniferaldehyde type groups after bleaching is higher for P-TMP than for B-TMP [25], this results in a higher amount of quinolic products formed by photoyellowing.

It does not implies that coniferaldehyde produce *o*-quinones upon oxidation. In fact, it is known that coniferaldehyde itself oxidizes by cleavage at the C_α-C_β link to give vanillin and a C_2 fragment. Also, it is believed that the usual precursors to quinones are phenoxy radicals [12]. But it may imply that phenolic hydroxyl and coniferaldehyde type groups are mainly involved in the structure of the *in situ* quinone precursors.

This residual amount of phenolic hydroxyl and coniferaldehyde type groups also explains the faster reaction rate [k_3] observed for P-TMP than for B-TMP, and that the minimum of the curves in Figure 9 comes sooner for P-TMP (3 min) than for B-TMP (4 min). This analysis would have been impossible if we only looked at ISO brightness and CIE L*a*b* coordinates.

By extrapolating from our results and if the relationship indicated by the dashed lines in Eq. *14 and 15* is right, we propose the following relationships between the chromophores involved in our experiments for the yellowing of thick handsheets (200 g/m^2):

$$C^{I}_{360} \longrightarrow C^{I}_{425} \qquad (16)$$

$$E \longrightarrow C^{II}_{360} \xrightarrow[\text{B-TMP}]{\text{P-TMP}} C^{II}_{425} \qquad (17)$$

$$C^{II}_{360} \xrightarrow{\text{TMP}} F \xrightarrow{} C^{II}_{425}$$

Conclusions

The results presented in this paper suggest that at least four (4) chromophores are involved in the yellowing of thick handsheets of black spruce/balsam fir TMP. A very fast reaction involved the disappearance of one chromophore around 360 nm

and the indirect creation of another chromophore around 425 nm (Eq. *16*). This fast reaction involves a chromophore that is affected by peroxide and borohydride bleaching in analog ways. This indicates that oxidation or reduction of this C^{I}_{360} chromophore eliminates its role in color reversion.

The identification of the unknown chemical "E" that may be responsible for the creation of C^{I}_{425} after UV irradiation of pulps (Eq. *17*), may indicate a way to prevent color reversion.

Works remain to be done to analyze other pulps treated with various chemicals to identify the structure of the chromophores involved. A complete comparison of the yellowing kinetics of various basis weight samples should also be undertaken. In this way, it will probably be possible to link these kinetics equations to the chemical structures recently proposed in the literature for the formation of arylglycerol-β-arylether ketyl radicals and their subsequent cleavage to form phenoxy radicals and aromatic ketones [12].

Acknowledgments

The authors thank the Natural Sciences and Engineering Research Council (Ottawa, Canada) and the Mechanical and Chemimechanical Wood-Pulp Network of Centers of Excellence for their financial support.

Literature Cited

1. S. E. Lebo, W. F. W. Lonsky, T. J. McDonough, P. J. Medvecz, Intl. Pulp Bleaching Conf, 247 (1988)
2. G. F. Leary, Tappi J., 50:1, 17 (1967)
3. S. Y. Lin and K. P. Kringstad, Tappi J., 53:4, 658 (1970)
4. K. P. Kringstad and S. Y. Lin, Tappi J., 53:12, 2296 (1970)
5. G. Brunow and M. Sivonen, Paperi Ja Puu, 4a, 215 (1975)
6. T. Matsuura, N. Yoshimura, A. Nishinaga and I. Saito, Tetrahedron, 28, 4933 (1972)
7. J. Gierer and S. Y. Lin, Svensk Papperstidning, 75:7, 233 (1972)

8. J.A. Schmidt, C. Heitner, 6 th Intl. Symp. Wood & Pulp. Chem., 263, (1991)

9. D.G. Holah, C. Heitner, Intl. Mech. Pulp. Conference, 177, (1991)

10. B. Holbom, R. Sjöholm, N. Åkerback, 6 th Intl. Symp. Wood & Pulp. Chem., 443, (1991)

11. J.C. Scaiano, J.C. Netto-Ferreira, V., Wintgens, J. Photochem. Photobiol. A: Chem., 59, 265 (1991)

12. J.A. Schmidt, C. Heitner, J. Wood Chem. Technol., 13:3, 309 (1993)

13. R.W. Johnson, Tappi J., 72:12, 181 (1989)

14. R.W. Kessler, G. Krablicher, S. Uhl, D. Oelkrug, W.P. Hagan, J. Hyslop, F, Wilkinson, Opt. Acta, 30, 1099 (1983)

15. D. Oelkrug, W. Honnen, F. Wilkinson, W.J. Willsher, J. Chem. Soc., Faraday Trans. 2, 83, 2081 (1987)

16. J.A. Schmidt, C. Heitner, G.P. Kelly, P.A. Leicester, F. Wilkinson, J. Photochem. Photobiol. A: Chem., 57, 111 (1991)

17. C. Heitner, J.A. Schmidt, 6 th Intl. Symp. Wood & Pulp. Chem., 131, (1991)

18. C. Heitner, T. Min, Cellulose Chem. Technol, 21:3, 289 (1987)

19. P. Fornier de Violet, A. Nourmamode, N. Columbo, A. Castellan, Cellulose Chem. Technol., 23:5, 535 (1989)

20. J.A. Schmidt, C. Heitner, J. Wood Chem. Technol., 11:4, 397 (1991)

21. R.C. Francis, C.W. Dence, T.C. Alexander, R. Agnemo, S. Omori, Tappi J., 74:12, 127 (1991)

22. D.W. Marquardt, J. Soc. Indust. Appl. Math., 11:2, 431 (1963)

23. S. Claesson, E. Olson, A. Wennerblom, Svensk Papperstidn., 71, 335 (1968)

24. I. Forsskåhl, J. Janson, 6 th Intl. Symp. Wood & Pulp. Chem., 255, (1991)

25. R.C. Francis, Y.Z. Lai, C.W. Dence, T.C. Alexander, Tappi J., 74:9, 219 (1991)